Supplemental Material for "Observation of Three Charmonium-Like States with $J^{PC} = 1^{--}$ in $e^+e^- \to D^{*0}D^{*-}\pi^+$"

M. Ablikim[1], M. N. Achasov[13,b], P. Adlarson[73], R. Aliberti[34], A. Amoroso[72A,72C], M. R. An[38], Q. An[69,56], Y. Bai[55], O. Bakina[35], I. Balossino[29A], Y. Ban[45,g], V. Batozskaya[1,43], K. Begzsuren[31], N. Berger[34], M. Bertani[28A], D. Bettoni[29A], F. Bianchi[72A,72C], E. Bianco[72A,72C], J. Bloms[66], A. Bortone[72A,72C], I. Boyko[35], R. A. Briere[5], A. Brueggemann[66], H. Cai[74], X. Cai[1,56], A. Calcaterra[28A], G. F. Cao[1,61], N. Cao[1,61], S. A. Cetin[60A], J. F. Chang[1,56], T. T. Chang[75], W. L. Chang[1,61], G. R. Che[42], G. Chelkov[35,a], C. Chen[42], Chao Chen[53], G. Chen[1], H. S. Chen[1,61], M. L. Chen[1,56,61], S. J. Chen[41], S. M. Chen[59], T. Chen[1,61], X. R. Chen[30,61], X. T. Chen[1,61], Y. B. Chen[1,56], Y. Q. Chen[33], Z. J. Chen[25,h], W. S. Cheng[72C], S. K. Choi[10A], X. Chu[42], G. Cibinetto[29A], S. C. Coen[4], F. Cossio[72C], J. J. Cui[48], H. L. Dai[1,56], J. P. Dai[77], A. Dbeyssi[19], R. E. de Boer[4], D. Dedovich[35], Z. Y. Deng[1], A. Denig[34], I. Denysenko[35], M. Destefanis[72A,72C], F. De Mori[72A,72C], B. Ding[64,1], X. X. Ding[45,g], Y. Ding[39], Y. Ding[33], J. Dong[1,56], L. Y. Dong[1,61], M. Y. Dong[1,56,61], X. Dong[74], S. X. Du[79], Z. H. Duan[41], P. Egorov[35,a], Y. L. Fan[74], J. Fang[1,56], S. S. Fang[1,61], W. X. Fang[1], Y. Fang[1], R. Farinelli[29A], L. Fava[72B,72C], F. Feldbauer[4], G. Felici[28A], C. Q. Feng[69,56], J. H. Feng[57], K Fischer[67], M. Fritsch[4], C. Fritzsch[66], C. D. Fu[1], Y. W. Fu[1], H. Gao[61], Y. N. Gao[45,g], Yang Gao[69,56], S. Garbolino[72C], I. Garzia[29A,29B], P. T. Ge[74], Z. W. Ge[41], C. Geng[57], E. M. Gersabeck[65], A Gilman[67], K. Goetzen[14], L. Gong[39], W. X. Gong[1,56], W. Gradl[34], S. Gramigna[29A,29B], M. Greco[72A,72C], M. H. Gu[1,56], Y. T. Gu[16], C. Y Guan[1,61], Z. L. Guan[22], A. Q. Guo[30,61], L. B. Guo[40], R. P. Guo[47], Y. P. Guo[12,f], A. Guskov[35,a], X. T. H.[1,61], W. Y. Han[38], X. Q. Hao[20], F. A. Harris[63], K. K. He[53], K. L. He[1,61], F. H. Heinsius[4], C. H. Heinz[34], Y. K. Heng[1,56,61], C. Herold[58], T. Holtmann[4], P. C. Hong[12,f], G. Y. Hou[1,61], Y. R. Hou[61], Z. L. Hou[1], H. M. Hu[1,61], J. F. Hu[54,i], T. Hu[1,56,61], Y. Hu[1], G. S. Huang[69,56], K. X. Huang[57], L. Q. Huang[30,61], X. T. Huang[48], Y. P. Huang[1], T. Hussain[71], N Hüsken[27,34], W. Imoehl[27], M. Irshad[69,56], J. Jackson[27], S. Jaeger[4], S. Janchiv[31], J. H. Jeong[10A], Q. Ji[1], Q. P. Ji[20], X. B. Ji[1,61], X. L. Ji[1,56], Y. Y. Ji[48], Z. K. Jia[69,56], P. C. Jiang[45,g], S. S. Jiang[38], T. J. Jiang[17], X. S. Jiang[1,56,61], Y. Jiang[61], J. B. Jiao[48], Z. Jiao[23], S. Jin[41], Y. Jin[64], M. Q. Jing[1,61], T. Johansson[73], X. K.[1], S. Kabana[32], N. Kalantar-Nayestanaki[62], X. L. Kang[9], X. S. Kang[39], R. Kappert[62], M. Kavatsyuk[62], B. C. Ke[79], A. Khoukaz[66], R. Kiuchi[1], R. Kliemt[14], L. Koch[36], O. B. Kolcu[60A], B. Kopf[4], M. Kuessner[4], A. Kupsc[43,73], W. Kühn[36], J. J. Lane[65], J. S. Lange[36], P. Larin[19], A. Lavania[26], L. Lavezzi[72A,72C], T. T. Lei[69,k], Z. H. Lei[69,56], H. Leithoff[34], M. Lellmann[34], T. Lenz[34], C. Li[46], C. Li[42], C. H. Li[38], Cheng Li[69,56], D. M. Li[79], F. Li[1,56], G. Li[1], H. Li[69,56], H. B. Li[1,61], H. J. Li[20], H. N. Li[54,i], Hui Li[42], J. R. Li[59], J. S. Li[57], J. W. Li[48], Ke Li[1], L. J Li[1,61], L. K. Li[1], Lei Li[3], M. H. Li[42], P. R. Li[37,j,k], S. X. Li[12], T. Li[48], W. D. Li[1,61], W. G. Li[1], X. H. Li[69,56], X. L. Li[48], Xiaoyu Li[1,61], Y. G. Li[45,g], Z. J. Li[57], Z. X. Li[16], Z. Y. Li[57], C. Liang[41], H. Liang[69,56], H. Liang[33], H. Liang[1,61], Y. F. Liang[52], Y. T. Liang[30,61], G. R. Liao[15], L. Z. Liao[48], J. Libby[26], A. Limphirat[58], D. X. Lin[30,61], T. Lin[1], B. X. Liu[74], B. J. Liu[1], C. Liu[33], C. X. Liu[1], D. Liu[19,69], F. H. Liu[51], Fang Liu[1], Feng Liu[6], G. M. Liu[54,i], H. Liu[37,j,k], H. B. Liu[16], H. M. Liu[1,61], Huanhuan Liu[1], Huihui Liu[21], J. B. Liu[69,56], J. L. Liu[70], J. Y. Liu[1,61], K. Liu[1], K. Y. Liu[39], Ke Liu[22], L. Liu[69,56], L. C. Liu[42], Lu Liu[42], M. H. Liu[12,f], P. L. Liu[1], Q. Liu[61], S. B. Liu[69,56], T. Liu[12,f], W. K. Liu[42], W. M. Liu[69,56], X. Liu[37,j,k], Y. Liu[37,j,k], Y. B. Liu[42], Z. A. Liu[1,56,61], Z. Q. Liu[48], X. C. Lou[1,56,61], F. X. Lu[57], H. J. Lu[23], J. G. Lu[1,56], X. L. Lu[1], Y. Lu[7], Y. P. Lu[1,56], Z. H. Lu[1,61], C. L. Luo[40], M. X. Luo[78], T. Luo[12,f], X. L. Luo[1,56], X. R. Lyu[61], Y. F. Lyu[42], F. C. Ma[39], H. L. Ma[1], J. L. Ma[1,61], L. L. Ma[48], M. M. Ma[1,61], Q. M. Ma[1], R. Q. Ma[1,61], R. T. Ma[61], X. Y. Ma[1,56], Y. Ma[45,g], F. E. Maas[19], M. Maggiora[72A,72C], S. Maldaner[4], S. Malde[67], A. Mangoni[28B], Y. J. Mao[45,g], Z. P. Mao[1], S. Marcello[72A,72C], Z. X. Meng[64], J. G. Messchendorp[14,62], G. Mezzadri[29A], H. Miao[1,61], T. J. Min[41], R. E. Mitchell[27], X. H. Mo[1,56,61], N. Yu. Muchnoi[13,b], Y. Nefedov[35], F. Nerling[19,d], I. B. Nikolaev[13,b], Z. Ning[1,56], S. Nisar[11,l], Y. Niu [48], S. L. Olsen[61], Q. Ouyang[1,56,61], S. Pacetti[28B,28C], X. Pan[53], Y. Pan[55], A. Pathak[33], Y. P. Pei[69,56], M. Pelizaeus[4], H. P. Peng[69,56], K. Peters[14,d], J. L. Ping[40], R. G. Ping[1,61], S. Plura[34], S. Pogodin[35], V. Prasad[32], F. Z. Qi[1], H. Qi[69,56], H. R. Qi[59], M. Qi[41], T. Y. Qi[12,f], S. Qian[1,56], W. B. Qian[61], C. F. Qiao[61], J. J. Qin[70], L. Q. Qin[15], X. P. Qin[12,f], X. S. Qin[48], Z. H. Qin[1,56], J. F. Qiu[1], S. Q. Qu[59], C. F. Redmer[34], K. J. Ren[38], A. Rivetti[72C], V. Rodin[62], M. Rolo[72C], G. Rong[1,61], Ch. Rosner[19], S. N. Ruan[42], N. Salone[43], A. Sarantsev[35,c], Y. Schelhaas[34], K. Schoenning[73], M. Scodeggio[29A,29B], K. Y. Shan[12,f], W. Shan[24], X. Y. Shan[69,56], J. F. Shangguan[53], L. G. Shao[1,61], M. Shao[69,56], C. P. Shen[12,f], H. F. Shen[1,61], W. H. Shen[61], X. Y. Shen[1,61], B. A. Shi[61], H. C. Shi[69,56], J. Y. Shi[1], Q. Q. Shi[53], R. S. Shi[1,61], X. Shi[1,56], J. J. Song[20], T. Z. Song[57], W. M. Song[33,1], Y. X. Song[45,g], S. Sosio[72A,72C], S. Spataro[72A,72C], F. Stieler[34], Y. J. Su[61], G. B. Sun[74], G. X. Sun[1], H. Sun[61], H. K. Sun[1], J. F. Sun[20], K. Sun[59], L. Sun[74], S. S. Sun[1,61], T. Sun[1,61], W. Y. Sun[33], Y. Sun[9], Y. J. Sun[69,56], Y. Z. Sun[1], Z. T. Sun[48], Y. X. Tan[69,56], C. J. Tang[52], G. Y. Tang[1], J. Tang[57], Y. A. Tang[74], L. Y Tao[70], Q. T. Tao[25,h], M. Tat[67], J. X. Teng[69,56], V. Thoren[73], W. H. Tian[57], W. H. Tian[50], Y. Tian[30,61], Z. F. Tian[74], I. Uman[60B], B. Wang[1], B. L. Wang[61], Bo Wang[69,56], C. W. Wang[41], D. Y. Wang[45,g], F. Wang[70], H. J. Wang[37,j,k], H. P. Wang[1,61], K. Wang[1,56], L. L. Wang[1], M. Wang[48], Meng Wang[1,61], S. Wang[12,f], T. Wang[12,f], T. J. Wang[42], W. Wang[57], W. Wang[70], W. H. Wang[74], W. P. Wang[69,56], X. Wang[45,g], X. F. Wang[37,j,k], X. J. Wang[38], X. L. Wang[12,f], Y. Wang[59], Y. D. Wang[44], Y. F. Wang[1,56,61], Y. H. Wang[46], Y. N. Wang[44], Y. Q. Wang[1], Yaqian Wang[18,1], Yi Wang[59], Z. Wang[1,56], Z. L. Wang[70], Z. Y. Wang[1,61], Ziyi Wang[61], D. Wei[68], D. H. Wei[15], F. Weidner[66], S. P. Wen[1], C. W. Wenzel[4], U. Wiedner[4], G. Wilkinson[67], M. Wolke[73], L. Wollenberg[4], C. Wu[38], J. F. Wu[1,61], L. H. Wu[1], L. J. Wu[1,61], X. Wu[12,f], X. H. Wu[33], Y. Wu[69], Y. J Wu[30], Z. Wu[1,56], L. Xia[69,56], X. M. Xian[38], T. Xiang[45,g], D. Xiao[37,j,k], G. Y. Xiao[41], H. Xiao[12,f], S. Y. Xiao[1], Y. L. Xiao[12,f], Z. J. Xiao[40], C. Xie[41], X. H. Xie[45,g], Y. Xie[48], Y. G. Xie[1,56], Y. H. Xie[6], Z. P. Xie[69,56], T. Y. Xing[1,61], C. F. Xu[1,61], C. J. Xu[57], G. F. Xu[1], H. Y. Xu[64], Q. J. Xu[17], W. L. Xu[64], X. P. Xu[53], Y. C. Xu[76], Z. P. Xu[41], Z. S. Xu[61], F. Yan[12,f], L. Yan[12,f], W. B. Yan[69,56], W. C. Yan[79], X. Q Yan[1], H. J. Yang[49,e], H. L. Yang[33], H. X. Yang[1], Tao Yang[1], Y. Yang[12,f], Y. F. Yang[42], Y. X. Yang[1,61], Yifan Yang[1,61], M. Ye[1,56], M. H. Ye[8], J. H. Yin[1], Z. Y. You[57], B. X. Yu[1,56,61], C. X. Yu[42], G. Yu[1,61], T. Yu[70], X. D. Yu[45,g], C. Z. Yuan[1,61], L. Yuan[2], S. C. Yuan[1], X. Q. Yuan[1], Y. Yuan[1,61], Z. Y. Yuan[57], C. X. Yue[38], A. A. Zafar[71], F. R. Zeng[48],

X. Zeng[12,f], Y. Zeng[25,h], Y. J. Zeng[1,61], X. Y. Zhai[33], Y. H. Zhan[57], A. Q. Zhang[1,61], B. L. Zhang[1,61], B. X. Zhang[1], D. H. Zhang[42], G. Y. Zhang[20], H. Zhang[69], H. H. Zhang[33], H. H. Zhang[57], H. Q. Zhang[1,56,61], H. Y. Zhang[1,56], J. J. Zhang[50], J. L. Zhang[75], J. Q. Zhang[40], J. W. Zhang[1,56,61], J. X. Zhang[37,j,k], J. Y. Zhang[1], J. Z. Zhang[1,61], Jiawei Zhang[1,61], L. M. Zhang[59], L. Q. Zhang[57], Lei Zhang[41], P. Zhang[1], Q. Y. Zhang[38,79], Shuihan Zhang[1,61], Shulei Zhang[25,h], X. D. Zhang[44], X. M. Zhang[1], X. Y. Zhang[53], X. Y. Zhang[48], Y. Zhang[67], Y. T. Zhang[79], Y. H. Zhang[1,56], Yan Zhang[69,56], Yao Zhang[1], Z. H. Zhang[1], Z. L. Zhang[33], Z. Y. Zhang[74], Z. Y. Zhang[42], G. Zhao[1], J. Zhao[38], J. Y. Zhao[1,61], J. Z. Zhao[1,56], Lei Zhao[69,56], Ling Zhao[1], M. G. Zhao[42], S. J. Zhao[79], Y. B. Zhao[1,56], Y. X. Zhao[30,61], Z. G. Zhao[69,56], A. Zhemchugov[35,a], B. Zheng[70], J. P. Zheng[1,56], W. J. Zheng[1,61], Y. H. Zheng[61], B. Zhong[40], X. Zhong[57], H. Zhou[48], L. P. Zhou[1,61], X. Zhou[74], X. K. Zhou[6], X. R. Zhou[69,56], X. Y. Zhou[38], Y. Z. Zhou[12,f], J. Zhu[42], K. Zhu[1], K. J. Zhu[1,56,61], L. Zhu[33], L. X. Zhu[61], S. H. Zhu[68], S. Q. Zhu[41], T. J. Zhu[12,f], W. J. Zhu[12,f], Y. C. Zhu[69,56], Z. A. Zhu[1,61], J. H. Zou[1], J. Zu[69,56]

(BESIII Collaboration)

[1] *Institute of High Energy Physics, Beijing 100049, People's Republic of China*
[2] *Beihang University, Beijing 100191, People's Republic of China*
[3] *Beijing Institute of Petrochemical Technology, Beijing 102617, People's Republic of China*
[4] *Bochum Ruhr-University, D-44780 Bochum, Germany*
[5] *Carnegie Mellon University, Pittsburgh, Pennsylvania 15213, USA*
[6] *Central China Normal University, Wuhan 430079, People's Republic of China*
[7] *Central South University, Changsha 410083, People's Republic of China*
[8] *China Center of Advanced Science and Technology, Beijing 100190, People's Republic of China*
[9] *China University of Geosciences, Wuhan 430074, People's Republic of China*
[10] *Chung-Ang University, Seoul, 06974, Republic of Korea*
[11] *COMSATS University Islamabad, Lahore Campus, Defence Road, Off Raiwind Road, 54000 Lahore, Pakistan*
[12] *Fudan University, Shanghai 200433, People's Republic of China*
[13] *G.I. Budker Institute of Nuclear Physics SB RAS (BINP), Novosibirsk 630090, Russia*
[14] *GSI Helmholtzcentre for Heavy Ion Research GmbH, D-64291 Darmstadt, Germany*
[15] *Guangxi Normal University, Guilin 541004, People's Republic of China*
[16] *Guangxi University, Nanning 530004, People's Republic of China*
[17] *Hangzhou Normal University, Hangzhou 310036, People's Republic of China*
[18] *Hebei University, Baoding 071002, People's Republic of China*
[19] *Helmholtz Institute Mainz, Staudinger Weg 18, D-55099 Mainz, Germany*
[20] *Henan Normal University, Xinxiang 453007, People's Republic of China*
[21] *Henan University of Science and Technology, Luoyang 471003, People's Republic of China*
[22] *Henan University of Technology, Zhengzhou 450001, People's Republic of China*
[23] *Huangshan College, Huangshan 245000, People's Republic of China*
[24] *Hunan Normal University, Changsha 410081, People's Republic of China*
[25] *Hunan University, Changsha 410082, People's Republic of China*
[26] *Indian Institute of Technology Madras, Chennai 600036, India*
[27] *Indiana University, Bloomington, Indiana 47405, USA*
[28] *INFN Laboratori Nazionali di Frascati , (A)INFN Laboratori Nazionali di Frascati, I-00044, Frascati, Italy; (B)INFN Sezione di Perugia, I-06100, Perugia, Italy; (C)University of Perugia, I-06100, Perugia, Italy*
[29] *INFN Sezione di Ferrara, (A)INFN Sezione di Ferrara, I-44122, Ferrara, Italy; (B)University of Ferrara, I-44122, Ferrara, Italy*
[30] *Institute of Modern Physics, Lanzhou 730000, People's Republic of China*
[31] *Institute of Physics and Technology, Peace Avenue 54B, Ulaanbaatar 13330, Mongolia*
[32] *Instituto de Alta Investigación, Universidad de Tarapacá, Casilla 7D, Arica, Chile*
[33] *Jilin University, Changchun 130012, People's Republic of China*
[34] *Johannes Gutenberg University of Mainz, Johann-Joachim-Becher-Weg 45, D-55099 Mainz, Germany*
[35] *Joint Institute for Nuclear Research, 141980 Dubna, Moscow region, Russia*
[36] *Justus-Liebig-Universitaet Giessen, II. Physikalisches Institut, Heinrich-Buff-Ring 16, D-35392 Giessen, Germany*
[37] *Lanzhou University, Lanzhou 730000, People's Republic of China*
[38] *Liaoning Normal University, Dalian 116029, People's Republic of China*
[39] *Liaoning University, Shenyang 110036, People's Republic of China*
[40] *Nanjing Normal University, Nanjing 210023, People's Republic of China*
[41] *Nanjing University, Nanjing 210093, People's Republic of China*
[42] *Nankai University, Tianjin 300071, People's Republic of China*
[43] *National Centre for Nuclear Research, Warsaw 02-093, Poland*
[44] *North China Electric Power University, Beijing 102206, People's Republic of China*
[45] *Peking University, Beijing 100871, People's Republic of China*
[46] *Qufu Normal University, Qufu 273165, People's Republic of China*
[47] *Shandong Normal University, Jinan 250014, People's Republic of China*
[48] *Shandong University, Jinan 250100, People's Republic of China*
[49] *Shanghai Jiao Tong University, Shanghai 200240, People's Republic of China*

[50] Shanxi Normal University, Linfen 041004, People's Republic of China
[51] Shanxi University, Taiyuan 030006, People's Republic of China
[52] Sichuan University, Chengdu 610064, People's Republic of China
[53] Soochow University, Suzhou 215006, People's Republic of China
[54] South China Normal University, Guangzhou 510006, People's Republic of China
[55] Southeast University, Nanjing 211100, People's Republic of China
[56] State Key Laboratory of Particle Detection and Electronics, Beijing 100049, Hefei 230026, People's Republic of China
[57] Sun Yat-Sen University, Guangzhou 510275, People's Republic of China
[58] Suranaree University of Technology, University Avenue 111, Nakhon Ratchasima 30000, Thailand
[59] Tsinghua University, Beijing 100084, People's Republic of China
[60] Turkish Accelerator Center Particle Factory Group, (A)Istinye University, 34010, Istanbul, Turkey; (B)Near East University, Nicosia, North Cyprus, 99138, Mersin 10, Turkey
[61] University of Chinese Academy of Sciences, Beijing 100049, People's Republic of China
[62] University of Groningen, NL-9747 AA Groningen, The Netherlands
[63] University of Hawaii, Honolulu, Hawaii 96822, USA
[64] University of Jinan, Jinan 250022, People's Republic of China
[65] University of Manchester, Oxford Road, Manchester, M13 9PL, United Kingdom
[66] University of Muenster, Wilhelm-Klemm-Strasse 9, 48149 Muenster, Germany
[67] University of Oxford, Keble Road, Oxford OX13RH, United Kingdom
[68] University of Science and Technology Liaoning, Anshan 114051, People's Republic of China
[69] University of Science and Technology of China, Hefei 230026, People's Republic of China
[70] University of South China, Hengyang 421001, People's Republic of China
[71] University of the Punjab, Lahore-54590, Pakistan
[72] University of Turin and INFN, (A)University of Turin, I-10125, Turin, Italy; (B)University of Eastern Piedmont, I-15121, Alessandria, Italy; (C)INFN, I-10125, Turin, Italy
[73] Uppsala University, Box 516, SE-75120 Uppsala, Sweden
[74] Wuhan University, Wuhan 430072, People's Republic of China
[75] Xinyang Normal University, Xinyang 464000, People's Republic of China
[76] Yantai University, Yantai 264005, People's Republic of China
[77] Yunnan University, Kunming 650500, People's Republic of China
[78] Zhejiang University, Hangzhou 310027, People's Republic of China
[79] Zhengzhou University, Zhengzhou 450001, People's Republic of China

[a] Also at the Moscow Institute of Physics and Technology, Moscow 141700, Russia
[b] Also at the Novosibirsk State University, Novosibirsk, 630090, Russia
[c] Also at the NRC "Kurchatov Institute", PNPI, 188300, Gatchina, Russia
[d] Also at Goethe University Frankfurt, 60323 Frankfurt am Main, Germany
[e] Also at Key Laboratory for Particle Physics, Astrophysics and Cosmology, Ministry of Education; Shanghai Key Laboratory for Particle Physics and Cosmology; Institute of Nuclear and Particle Physics, Shanghai 200240, People's Republic of China
[f] Also at Key Laboratory of Nuclear Physics and Ion-beam Application (MOE) and Institute of Modern Physics, Fudan University, Shanghai 200443, People's Republic of China
[g] Also at State Key Laboratory of Nuclear Physics and Technology, Peking University, Beijing 100871, People's Republic of China
[h] Also at School of Physics and Electronics, Hunan University, Changsha 410082, China
[i] Also at Guangdong Provincial Key Laboratory of Nuclear Science, Institute of Quantum Matter, South China Normal University, Guangzhou 510006, China
[j] Also at Frontiers Science Center for Rare Isotopes, Lanzhou University, Lanzhou 730000, People's Republic of China
[k] Also at Lanzhou Center for Theoretical Physics, Lanzhou University, Lanzhou 730000, People's Republic of China
[l] Also at the Department of Mathematical Sciences, IBA, Karachi , Pakistan

(Dated: **March 14, 2023)**

I. DETAILS ON EVENT SELECTION

Two-dimensional distributions of $P^*(\pi^0)$ versus $M(\pi^0 D)$ for MC samples with D^0tag and D^-tag methods at $\sqrt{s} = 4.600\,\mathrm{GeV}$ are shown in Fig. 1, respectively.

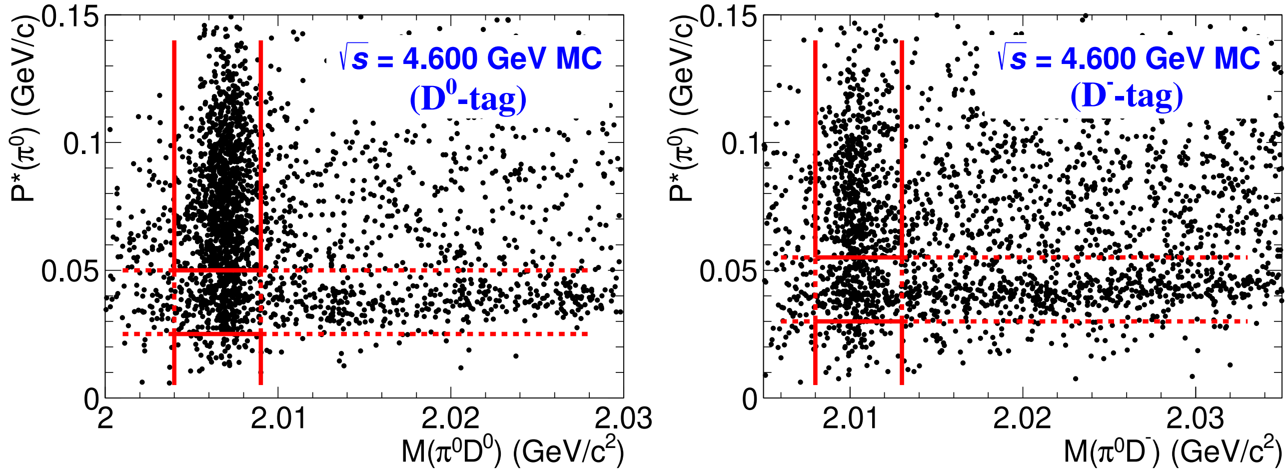

FIG. 1. Two-dimensions distributions of $P^*(\pi^0)$ versus $M(\pi^0 D)$ for MC simulation with D^0tag and D^-tag methods at $\sqrt{s} = 4.600\,\text{GeV}$. The events are kept inside the vertical solid lines and vetoed inside the horizontal dashed lines based on the requirements for $M(\pi^0 D)$ and $P^*(\pi^0)$.

II. SIGNAL YIELDS AND BORN CROSS SECTION

A simultaneous fit of D^0tag and D^-tag is performed at each energy point according to the calculation of the Born cross section.

$$\sigma^{\text{Born}} = \frac{\sigma^{\text{dressed}}}{\frac{1}{|1-\Pi|^2}} = \frac{N^{\text{obs}}_{D^{0(-)}\text{tag}}}{\mathcal{L}_{\text{int}}\epsilon_{D^{0(-)}\text{tag}}\hat{\mathcal{B}}_{D^{0(-)}\text{tag}}(1+\delta^{\text{ISR}})\frac{1}{|1-\Pi|^2}}.$$

The integral luminosities $\mathcal{L}_{\text{int}}$ are measured by Refs. [1–3]. The σ^{Born} is taken as a common parameter in the fitting while detection efficiencies, ISR and vacuum polarization factors are estimated based on MC simulation. With the fit results shown in Tables I and II, $N^{\text{obs}}_{D^0\text{tag}}$ and $N^{\text{obs}}_{D^-\text{tag}}$ can be calculated directly.

TABLE I. The Born cross section of $e^+e^- \to D^{*0}D^{*-}\pi^+$ for XYZ data sets, where the charge conjugation mode is also included. The first uncertainties are statistical and the second ones systematic.

$\sqrt{s}$ (GeV)	$\mathcal{L}_{\rm int}$ (pb^{-1})	$1+\delta^{\rm ISR}$	$\frac{1}{\|1-\Pi\|^2}$	$N^{\rm obs}_{D^0{\rm tag}}$	$\epsilon_{D^0{\rm tag}}$ (%)	$N^{\rm obs}_{D^-{\rm tag}}$	$\epsilon_{D^-{\rm tag}}$ (%)	$\sigma^{\rm Born}$ (pb)
4.189	570.0	0.668	1.056	32.0 ± 5.5	1.1	8.3 ± 1.4	1.6	$44.9 \pm 7.8 \pm 3.5$
4.199	526.6	0.677	1.056	62.6 ± 8.6	2.0	13.4 ± 1.8	2.6	$48.5 \pm 6.7 \pm 3.8$
4.209	572.1	0.697	1.057	193.3 ± 14.2	2.9	37.5 ± 2.7	3.3	$94.4 \pm 6.9 \pm 7.5$
4.219	569.2	0.725	1.056	291.0 ± 17.1	3.6	55.0 ± 3.2	4.0	$110.2 \pm 6.5 \pm 8.7$
4.226	1111.9	0.749	1.056	1173.5 ± 42.1	4.3	173.9 ± 6.2	4.8	$145.6 \pm 5.2 \pm 11.5$
4.236	530.3	0.770	1.056	468.0 ± 24.1	4.2	88.5 ± 4.6	4.8	$151.7 \pm 7.8 \pm 11.5$
4.242	55.9	0.780	1.055	51.6 ± 8.9	5.4	9.7 ± 1.7	6.1	$122.3 \pm 21.2 \pm 8.5$
4.244	538.1	0.784	1.056	522.4 ± 26.6	5.3	98.5 ± 5.0	6.0	$130.4 \pm 6.6 \pm 9.0$
4.258	828.4	0.795	1.054	1077.9 ± 37.9	5.5	162.8 ± 5.7	6.2	$132.6 \pm 4.7 \pm 10.8$
4.267	531.1	0.799	1.053	571.3 ± 28.2	4.6	109.5 ± 5.4	5.3	$163.6 \pm 8.1 \pm 11.6$
4.278	175.7	0.803	1.053	177.7 ± 16.1	4.6	34.1 ± 3.1	5.2	$153.7 \pm 13.9 \pm 10.9$
4.287	494.2	0.803	1.053	578.5 ± 27.7	5.8	109.9 ± 5.3	6.5	$141.8 \pm 6.8 \pm 10.4$
4.308	45.1	0.802	1.052	85.0 ± 11.1	5.5	16.3 ± 2.1	6.3	$239.0 \pm 31.3 \pm 19.1$
4.311	494.3	0.802	1.052	745.5 ± 33.2	5.5	143.8 ± 6.4	6.3	$193.7 \pm 8.6 \pm 15.5$
4.337	506.1	0.798	1.051	1078.9 ± 42.2	7.4	201.5 ± 7.9	8.2	$203.7 \pm 8.0 \pm 19.6$
4.358	543.9	0.798	1.051	1604.8 ± 50.2	8.0	304.4 ± 9.5	9.0	$262.3 \pm 8.2 \pm 20.1$
4.377	524.7	0.795	1.051	1909.7 ± 55.2	6.0	367.6 ± 10.6	6.8	$431.5 \pm 12.5 \pm 35.9$
4.387	55.6	0.794	1.051	234.1 ± 19.2	7.8	45.2 ± 3.7	8.9	$384.3 \pm 31.5 \pm 28.0$
4.395	508.2	0.792	1.051	2421.6 ± 60.0	7.6	466.1 ± 11.5	8.7	$446.5 \pm 11.1 \pm 32.5$
4.416	1090.7	0.794	1.052	6225.0 ± 95.7	7.4	1185.2 ± 18.2	8.3	$547.7 \pm 8.4 \pm 38.5$
4.436	570.6	0.796	1.054	3798.9 ± 74.6	7.6	755.4 ± 14.8	9.0	$619.3 \pm 12.2 \pm 42.2$
4.467	111.1	0.810	1.055	929.9 ± 35.9	7.8	176.2 ± 6.8	8.8	$742.9 \pm 28.7 \pm 50.8$
4.527	112.1	0.863	1.054	1128.2 ± 39.2	8.4	217.5 ± 7.5	9.7	$776.7 \pm 27.0 \pm 60.5$
4.575	48.9	0.900	1.054	430.3 ± 25.1	10.2	86.1 ± 5.0	12.1	$537.1 \pm 31.4 \pm 36.4$
4.600	586.9	0.905	1.055	5964.6 ± 95.1	10.4	1206.9 ± 19.2	12.5	$606.4 \pm 9.7 \pm 41.2$
4.613	103.7	0.908	1.055	1019.2 ± 38.9	9.9	210.1 ± 8.0	12.1	$613.4 \pm 23.4 \pm 41.2$
4.628	521.5	0.903	1.054	5115.1 ± 88.6	10.2	1026.4 ± 17.8	12.1	$599.2 \pm 10.4 \pm 40.5$
4.641	551.7	0.900	1.054	5404.6 ± 90.2	10.0	1123.5 ± 18.7	12.4	$608.4 \pm 10.1 \pm 44.4$
4.661	529.4	0.893	1.054	5434.9 ± 91.8	10.1	1111.6 ± 18.8	12.2	$641.7 \pm 10.8 \pm 47.1$
4.682	1667.4	0.894	1.054	18143.7 ± 168.0	10.6	3743.9 ± 34.7	12.9	$647.2 \pm 6.0 \pm 45.3$
4.699	535.5	0.900	1.055	6088.0 ± 97.2	10.4	1265.0 ± 20.2	12.9	$680.3 \pm 10.9 \pm 48.9$
4.740	163.9	0.925	1.055	1761.7 ± 54.3	11.0	374.8 ± 11.5	13.9	$595.0 \pm 18.3 \pm 43.3$
4.750	366.6	0.934	1.055	3902.4 ± 80.9	11.0	824.4 ± 17.1	13.8	$580.0 \pm 12.0 \pm 40.9$
4.781	511.5	0.957	1.055	5185.2 ± 95.2	10.9	1113.7 ± 20.4	13.9	$546.8 \pm 10.0 \pm 36.6$
4.843	525.2	0.979	1.056	4539.6 ± 91.7	10.6	972.9 ± 19.7	13.4	$468.4 \pm 9.5 \pm 33.1$
4.918	207.8	0.973	1.056	1674.8 ± 55.2	10.4	370.3 ± 12.2	13.6	$448.7 \pm 14.8 \pm 31.8$
4.951	159.3	0.965	1.056	1273.9 ± 39.5	10.3	283.3 ± 8.8	13.5	$452.9 \pm 14.1 \pm 31.1$

TABLE II. The Born cross section of $e^+e^- \to D^{*0}D^{*-}\pi^+$ for Scan data sets, where the charge conjugation mode is also included. The first uncertainties are statistical and the second ones systematic.

$\sqrt{s}$ (GeV)	$\mathcal{L}_{\rm int}$ (pb^{-1})	$1+\delta^{\rm ISR}$	$\frac{1}{\lvert 1-\Pi\rvert^2}$	$N^{\rm obs}_{D^0{\rm tag}}$	$\epsilon_{D^0{\rm tag}}$ (%)	$N^{\rm obs}_{D^-{\rm tag}}$	$\epsilon_{D^-{\rm tag}}$ (%)	$\sigma^{\rm Born}$ (pb)
4.200	6.8	0.677	1.057	2.9 ± 1.8	2.3	0.6 ± 0.4	2.8	$156.2 \pm 94.9 \pm 12.3$
4.203	7.6	0.681	1.057	3.4 ± 1.9	2.5	0.7 ± 0.4	3.0	$146.3 \pm 82.4 \pm 11.6$
4.207	7.7	0.691	1.057	3.7 ± 2.1	2.9	0.7 ± 0.4	3.3	$134.3 \pm 78.2 \pm 10.6$
4.212	7.8	0.705	1.057	4.2 ± 2.2	3.2	0.8 ± 0.4	3.7	$134.6 \pm 69.6 \pm 10.6$
4.217	7.9	0.720	1.056	6.0 ± 2.5	3.8	1.1 ± 0.5	4.2	$158.1 \pm 65.7 \pm 12.5$
4.222	8.2	0.738	1.056	6.5 ± 3.1	4.0	1.2 ± 0.6	4.4	$150.2 \pm 70.8 \pm 11.9$
4.227	8.2	0.751	1.056	5.9 ± 2.6	4.2	1.1 ± 0.5	4.7	$128.8 \pm 56.6 \pm 10.2$
4.232	8.3	0.762	1.056	7.0 ± 3.0	4.2	1.3 ± 0.6	4.7	$148.8 \pm 64.0 \pm 11.8$
4.237	7.8	0.773	1.055	3.5 ± 2.9	5.0	0.7 ± 0.5	5.6	$65.0 \pm 53.7 \pm 4.5$
4.240	8.6	0.778	1.055	10.0 ± 4.1	5.2	1.8 ± 0.8	5.6	$163.5 \pm 67.2 \pm 11.3$
4.242	8.5	0.781	1.056	8.1 ± 3.3	5.5	1.5 ± 0.6	5.8	$125.4 \pm 51.2 \pm 8.7$
4.245	8.6	0.784	1.056	11.7 ± 3.7	5.5	2.2 ± 0.7	6.0	$179.1 \pm 57.1 \pm 12.4$
4.247	8.6	0.787	1.055	14.9 ± 3.7	5.6	2.7 ± 0.7	6.1	$219.5 \pm 55.3 \pm 15.2$
4.252	8.7	0.792	1.054	5.3 ± 2.9	5.3	1.0 ± 0.5	5.9	$81.9 \pm 45.1 \pm 6.7$
4.257	8.9	0.795	1.054	10.7 ± 4.3	5.4	2.1 ± 0.8	6.1	$157.6 \pm 62.8 \pm 12.8$
4.262	8.6	0.796	1.053	16.9 ± 3.9	4.6	3.2 ± 0.7	5.1	$300.1 \pm 68.9 \pm 21.2$
4.267	8.6	0.798	1.053	5.2 ± 3.4	4.7	1.0 ± 0.6	5.2	$90.8 \pm 60.1 \pm 6.4$
4.272	8.6	0.800	1.053	7.7 ± 3.2	4.7	1.5 ± 0.6	5.4	$133.5 \pm 55.9 \pm 9.4$
4.277	8.7	0.800	1.053	10.2 ± 4.3	5.9	1.9 ± 0.8	6.7	$139.0 \pm 57.7 \pm 9.8$
4.282	8.6	0.803	1.053	16.0 ± 3.9	6.1	3.0 ± 0.7	6.7	$214.0 \pm 52.4 \pm 15.7$
4.287	9.0	0.802	1.053	9.1 ± 4.0	6.1	1.7 ± 0.8	6.8	$117.6 \pm 51.4 \pm 8.6$
4.297	8.5	0.801	1.052	15.9 ± 4.9	5.5	2.9 ± 0.9	6.0	$242.0 \pm 74.9 \pm 19.3$
4.307	8.6	0.803	1.052	10.9 ± 4.2	5.4	2.1 ± 0.8	6.2	$163.2 \pm 62.5 \pm 13.0$
4.317	9.3	0.801	1.052	3.7 ± 3.6	5.9	0.8 ± 0.7	6.5	$53.4 \pm 46.1 \pm 4.3$
4.327	8.7	0.800	1.051	30.2 ± 6.9	7.4	5.7 ± 1.3	8.2	$333.1 \pm 75.9 \pm 32.0$
4.337	8.7	0.798	1.051	18.2 ± 6.0	7.4	3.4 ± 1.1	8.2	$199.9 \pm 65.6 \pm 19.2$
4.347	8.5	0.798	1.051	23.8 ± 6.4	7.8	4.3 ± 1.2	8.4	$251.9 \pm 68.0 \pm 19.3$
4.357	8.1	0.797	1.051	36.9 ± 7.2	7.6	6.9 ± 1.3	8.4	$428.1 \pm 83.0 \pm 32.8$
4.367	8.5	0.796	1.051	23.0 ± 7.2	6.1	4.2 ± 1.3	6.6	$316.5 \pm 99.5 \pm 26.3$
4.377	8.2	0.796	1.051	29.9 ± 7.1	6.2	5.7 ± 1.4	7.0	$421.9 \pm 99.7 \pm 35.1$
4.387	7.5	0.794	1.051	40.2 ± 8.1	7.9	7.3 ± 1.5	8.5	$487.6 \pm 98.4 \pm 35.5$
4.392	7.4	0.794	1.051	37.5 ± 7.7	7.9	7.2 ± 1.5	8.9	$454.6 \pm 93.3 \pm 33.1$
4.397	7.2	0.793	1.051	38.3 ± 7.8	8.0	7.2 ± 1.5	9.0	$471.3 \pm 96.1 \pm 34.3$
4.407	6.4	0.793	1.052	36.3 ± 7.7	7.3	6.9 ± 1.5	8.2	$558.4 \pm 118.7 \pm 39.2$
4.417	7.5	0.793	1.052	37.4 ± 8.2	7.5	7.1 ± 1.6	8.4	$473.1 \pm 103.7 \pm 33.2$
4.422	7.4	0.793	1.052	43.9 ± 8.2	7.4	8.3 ± 1.6	8.3	$564.9 \pm 106.1 \pm 39.7$
4.427	6.8	0.794	1.053	42.0 ± 8.0	8.7	8.1 ± 1.5	9.9	$503.3 \pm 95.9 \pm 34.3$
4.437	7.6	0.796	1.054	52.5 ± 9.3	8.0	10.3 ± 1.8	9.3	$609.9 \pm 108.1 \pm 41.6$
4.447	7.7	0.800	1.054	67.7 ± 9.8	7.3	12.8 ± 1.9	8.2	$845.9 \pm 123.1 \pm 57.7$
4.457	8.7	0.803	1.055	69.9 ± 10.3	7.4	13.5 ± 2.0	8.5	$756.7 \pm 111.1 \pm 51.7$
4.477	8.2	0.816	1.055	85.4 ± 11.0	7.9	15.6 ± 2.0	8.6	$909.9 \pm 117.0 \pm 62.2$
4.497	8.0	0.833	1.055	81.6 ± 10.8	7.9	15.6 ± 2.1	8.9	$874.1 \pm 116.0 \pm 59.7$
4.517	8.7	0.855	1.055	73.6 ± 10.8	8.2	13.9 ± 2.0	9.1	$682.5 \pm 100.3 \pm 53.2$
4.537	9.3	0.875	1.054	101.3 ± 12.3	9.4	20.1 ± 2.4	11.1	$739.8 \pm 89.7 \pm 57.6$
4.547	8.8	0.884	1.054	92.0 ± 11.8	9.6	18.2 ± 2.3	11.2	$697.0 \pm 89.7 \pm 54.3$
4.557	8.3	0.892	1.054	90.9 ± 11.3	9.8	17.9 ± 2.2	11.5	$704.7 \pm 87.8 \pm 47.8$
4.567	8.4	0.897	1.054	96.5 ± 12.3	9.8	19.0 ± 2.4	11.4	$737.6 \pm 94.2 \pm 50.0$
4.577	8.5	0.901	1.055	78.7 ± 11.3	9.7	15.8 ± 2.3	11.6	$591.7 \pm 84.7 \pm 40.1$
4.587	8.2	0.905	1.055	83.3 ± 11.6	9.9	16.6 ± 2.3	11.7	$639.5 \pm 89.1 \pm 43.4$

III. MULTIPLE SOLUTIONS OF LINESHAPE FIT

The dressed cross section is parameterized as the coherent sum of a continuum amplitude for $e^+e^- \to D^{*0}D^{*-}\pi^+$ and three $R_k \to D^{*0}D^{*-}\pi^+$ resonance amplitudes:

$$\sigma^{\text{dressed}}(\sqrt{s}) = C_0|C_1\sqrt{\Phi(\sqrt{s})} + \sum_{k=1}^{3} \text{BW}_k(\sqrt{s})e^{i\phi_k}|^2,$$

where the relativistic Breit-Wigner functions are given by

$$\text{BW}_k(\sqrt{s}) = \frac{m_k}{\sqrt{s}} \frac{\sqrt{12\pi\Gamma_k^{ee}\mathcal{B}_k\Gamma_k^{\text{tot}}}}{s - m_k^2 + im_k\Gamma_k^{\text{tot}}} \sqrt{\frac{\Phi(\sqrt{s})}{\Phi(m_k)}},$$

and the 3-body phase space contribution $\Phi(\sqrt{s}) = \iint \frac{1}{(2\pi)^3 32(\sqrt{s})^3} dm_{23}^2 dm_{12}^2$. All the parameters in the fit are free except for $C_0 = 3.894 \times 10^5\,\text{nb}\,\text{GeV}^2$ as a unit conversion factor.

In the above function, mathematically there exists eight solutions with the same outputs of the dressed cross sections [7], which is due to the interference between any two of the involved components in the fitting function. The different combinations of the amplitude and relative phase angle of each component can lead to the same outcome, whose sizes are presented by the parameters $\Gamma_k^{ee}\mathcal{B}_k$ and ϕ_k, respectively. This means that there are eight degenerate solutions with the same fit quality, as shown in Fig. 2. Among them, the results of the resonance masses m_k and total widths Γ_k^{tot} in the multiple solutions are equal, while those of the partial width and relative phase angle vary.

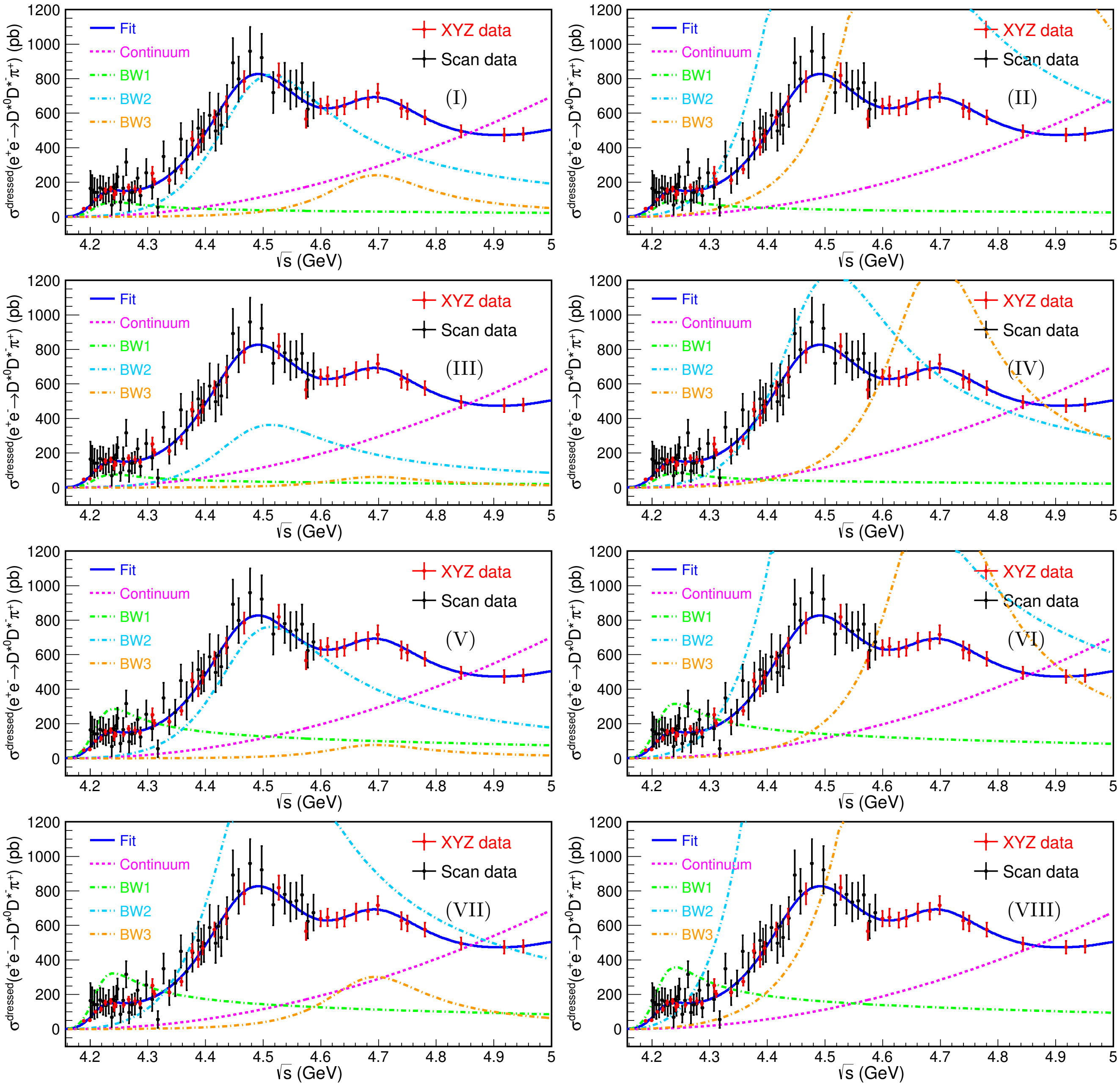

FIG. 2. The fit results of the dressed cross section lineshape of $e^+e^- \to D^{*0}D^{*-}\pi^+$, where the charge conjugation mode is also included. The black and red points with error bars are data, including statistical and systematic uncertainties. The blue curve is the total fit. The green, azure and orange dashed curves describe three BW functions, and the pink dashed-curve is the three body phase space contribution.

IV. SYSTEMATIC UNCERTAINTIES

The systematic uncertainty studies are performed at energy points where the signal yield is larger than 500 events. For other points suffering limited statistics, the uncertainty from the closest point is taken as its systematic uncertainty. All the systematic uncertainties are studied on each tag method separately and then combined together according to their yields. To consider all the related systematic uncertainties in the measurement of the Born cross sections, the sources of systematic uncertainty are divided into three categories.

The first category includes uncertainties associated with the detection efficiencies, such as tracking, particle identification, π^0 reconstruction, signal region requirements of the reconstructed unstable particles (*i.e.*, the $P^*(\pi^0)$ momentum rejection region, $D^0(D^-)$ and $D^{*0}(D^{*-})$ mass window requirements), MC simulation model and ISR correction factors. The uncertainty of detection and PID efficiency is 1.0% for each charged track [4], and 2.0% for π^0 reconstruction [5]. The uncertainties associated with the $P^*(\pi^0)$, $M(D^0(D^-))$ and $M(D^{*0}(D^{*-}))$ windows are estimated by re-extracting the detection efficiencies with Gaussian-smeared MC samples where the Gaussian parameters are obtained from the discrepancies between data and MC simulation. The MC samples are corrected according to the partial-wave-analysis (PWA) results at each energy point. To estimate the uncertainties from PWA-corrected MC samples, the samples with different PWA results are re-corrected by changing the possible components used in the PWA. The differences of efficiencies extracted from nominal and re-corrected MC samples are taken as the systematic uncertainty of the signal model. The ISR correction factors can have an impact on the detection efficiencies by affecting the slope of the lineshape, and hence, they are treated together as $(1+\delta^{\rm ISR})\epsilon$. Since the ISR correction factors are estimated by the fitting-iteration method, the uncertainty of this item comes from four different parts: the differences between the last two iterations are taken as the uncertainty of the iteration method itself; the uncertainty from the lineshape fitting model used in the iteration are estimated by replacing the phase space model with a parameterized function; the uncertainty of $(1+\delta^{\rm ISR})\epsilon$ is estimated by 500 groups of cross-section toys which are re-sampled according to the uncertainty of the parameters and the corresponding covariance matrix; the vacuum polarization factors are taken from QED calculations at each energy point and affect the slope of the lineshape with an estimated uncertainty of 0.5%.

The second category includes uncertainties associated with the signal shape, background shape and fit range, which affect the estimation of signal yields. The uncertainty of the signal shape is estimated by convolving it with a double-Gaussian function in the fit instead of a single Gaussian function in the nominal results. The description of the background shape is changed from a $2^{\rm nd}$ order Chebyshev function to a linear function in the fit and the differences between the two cases are considered as the uncertainty. The uncertainty associated with the fit range uncertainty is determined by altering the fit range from $(1.91, 2.12)\,{\rm GeV}/c^2$ to $(1.911, 2.12)\,{\rm GeV}/c^2$.

The last category includes the luminosity and quoted BFs, where the former uncertainty is 1.0% at each energy point [1–3], and the latter uncertainties are taken from the PDG [6].

Assuming no significant correlations between sources, the total systematic uncertainty is obtained as the sum in quadrature. Table III summarizes the systematic uncertainties of the cross section at various energy points.

TABLE III. The summary of all the systematic uncertainties (%) in the Born cross section measurement. The items marked with '†' are treated as fully correlated uncertainties, while others are uncorrelated uncertainties.

$\sqrt{s}$ (GeV)	Track†	PID†	$\pi^{0\dagger}$	Signal region	Decay Model	$(1+\delta^{\rm ISR})^{\dagger}$	Signal shape	Bkg. shape	Fit range	$\mathcal{L}_{\rm int}^{\dagger}$	$\mathcal{B}^{\dagger}$	Total
4.226	3.7	3.7	2.8	0.5	0.9	1.4	2.5	0.9	3.1	1.0	2.7	7.9
4.236	3.7	3.7	2.7	0.4	0.3	1.0	2.3	0.5	2.6	1.0	2.7	7.6
4.244	3.6	3.6	2.8	0.6	0.6	0.8	1.0	1.2	1.3	1.0	2.7	6.9
4.258	3.6	3.6	2.8	0.6	0.0	0.7	2.6	2.5	3.2	1.0	2.7	8.1
4.267	3.6	3.6	2.8	0.7	0.1	0.7	1.8	0.5	1.8	1.0	2.7	7.1
4.288	3.7	3.7	2.8	0.2	0.1	1.9	1.6	1.6	1.6	1.0	2.7	7.3
4.312	3.6	3.6	2.7	0.3	0.6	2.9	1.6	3.0	1.5	1.0	2.6	8.0
4.337	3.6	3.6	2.7	0.4	0.5	2.3	1.9	6.0	2.1	1.0	2.7	9.6
4.358	3.7	3.7	2.8	0.5	0.1	2.3	1.3	2.5	1.7	1.0	2.7	7.7
4.377	3.7	3.7	2.7	0.4	0.4	1.2	0.9	4.6	1.7	1.0	2.7	8.3
4.397	3.7	3.7	2.8	0.3	0.6	0.6	0.9	2.7	0.8	1.0	2.7	7.3
4.416	3.7	3.7	2.7	0.6	0.4	0.8	0.2	2.3	0.5	1.0	2.7	7.0
4.436	3.7	3.7	2.8	0.3	0.2	0.9	1.2	1.3	0.0	1.0	2.7	6.8
4.467	3.7	3.7	2.7	0.5	0.6	1.0	0.3	1.5	0.4	1.0	2.7	6.8
4.527	3.7	3.7	2.7	0.4	0.4	0.9	3.1	1.0	2.5	1.0	2.7	7.8
4.575	3.7	3.7	2.8	0.5	0.3	0.6	1.1	0.6	0.4	1.0	2.7	6.8
4.600	3.7	3.7	2.7	0.5	1.2	0.9	0.5	0.3	0.7	1.0	2.6	6.8
4.612	3.7	3.7	2.8	0.2	0.4	1.1	0.5	0.7	0.5	1.0	2.7	6.7
4.628	3.7	3.7	2.7	0.4	0.1	1.3	0.7	0.9	0.4	1.0	2.6	6.8
4.641	3.7	3.7	2.7	0.3	1.0	2.7	0.7	1.1	0.8	1.0	2.7	7.3
4.661	3.7	3.7	2.8	0.3	2.0	2.6	0.6	0.3	0.1	1.0	2.7	7.3
4.681	3.7	3.7	2.7	0.3	0.5	2.4	0.2	0.5	0.1	1.0	2.7	7.0
4.698	3.7	3.7	2.7	0.2	1.0	2.5	0.1	1.1	0.4	1.0	2.7	7.2
4.740	3.7	3.7	2.7	0.5	2.5	1.5	0.5	0.8	0.8	1.0	2.6	7.3
4.750	3.7	3.7	2.7	0.3	2.1	1.0	0.1	0.6	0.5	1.0	2.6	7.0
4.781	3.7	3.7	2.7	0.4	0.4	0.8	0.2	0.4	0.9	1.0	2.6	6.7
4.843	3.7	3.7	2.7	0.2	2.1	1.2	0.4	0.9	0.6	1.0	2.6	7.1
4.918	3.7	3.7	2.7	0.4	1.8	1.2	0.4	1.4	0.5	1.0	2.6	7.1
4.951	3.7	3.7	2.8	0.4	0.6	0.8	0.6	1.6	0.6	1.0	2.7	6.9

[1] M. Ablikim *et al.* (BESIII Collaboration), Chin. Phys. C **41**, 063001 (2017).
[2] M. Ablikim *et al.* (BESIII Collaboration), Chin. Phys. C **45**, 103001 (2021).
[3] M. Ablikim *et al.* (BESIII Collaboration), Chin. Phys. C **46**, 113003 (2022).
[4] M. Ablikim *et al.* (BESIII Collaboration), Phys. Rev. D **83**, 112005 (2011).
[5] M. Ablikim *et al.* (BESIII Collaboration), Phys. Rev. D **81**, 052005 (2010).
[6] R. L. Workman (Particle Data Group), PTEP **2022**, 083C01 (2022).
[7] Y. Bai and D. Y. Chen, Phys. Rev. D **99**, 072007 (2019).